Carbohydrate Polymers 90 (2012) 1330–1336

Contents lists available at SciVerse ScienceDirect

Carbohydrate Polymers

journal homepage: www.elsevier.com/locate/carbpol

Rheological properties of aqueous solution containing xanthan gum and cationic cellulose JR400

Haiping Li[a], Renfu Chen[b], Xiaomei Lu[a], Wanguo Hou[a,*]

[a] Key Laboratory for Colloid and Interface Chemistry of Education Ministry, Shandong University, Jinan 250100, PR China
[b] College Entrance Examination Tutorial Schools of Anqiu City, Anqiu 262100, PR China

ARTICLE INFO

Article history:
Received 23 May 2012
Received in revised form 25 June 2012
Accepted 2 July 2012
Available online 10 July 2012

Keywords:
Electrostatic attraction
Xanthan gum
JR400
Shear rate
pH
Electrolyte

ABSTRACT

Rheological properties of aqueous solution containing xanthan gum (XG) and cationic cellulose JR400 were investigated at different composition ratio, shear rate, pH and electrolyte concentrations. It was found that the mixing of XG and JR400 can induce a viscosity-increasing effect for the mixed solution. As the concentration fraction (f_{JR}) of JR400 in the mixed solution increases from 0 to 0.40 with the total polymer concentration (c_t) of 1%, the solution transforms from an elastic fluid into a viscoelastic one, while as f_{JR} decreases from 1 to 0.78, the solution transforms from a viscous fluid into a viscoelastic one. At pH 5–10, both the viscosity and elasticity of XG/JR400 mixture (f_{JR} = 0.15) are independent of pH and the viscosity-increasing effect is obvious. Outside this pH range, the viscosity, elasticity and viscosity-increasing effect of the mixture decrease. The increase of added NaCl concentration and shear rate can induce the decrease of viscosity, elasticity and viscosity-increasing effect of the XG/JR400 mixture.

1. Introduction

Polyelectrolyte complexes (PECs) can be formed via the electrostatic interaction between polyanions and polycations (Fuoss & Sadek, 1949; Michaels & Miekka, 1961; Michaels, Mir, & Schneider, 1965). Since the early work on PECs by Fuoss and Sadek (1949) and by Michaels and Miekka (1961), lots of studies and reviews have been published in this field (Al-Jamal, Ramaswamy, & Florence, 2005; Kötz, Kosmella, & Beitz, 2001; Kabanov & Kabanov, 1998; Kabanov, 2005; Michaels, 1965; Thünemann, Müller, Dautzenberg, Joanny, & Löwen, 2004; Tsuchida & Abe, 1982). PECs has been applied in many areas, such as coatings, binders (Doi & Kokufuta, 2010), flocculants (Dinu, Mihai, & Dragan, 2010), delivery and controlled release of drug (El-Hag Ali Said, 2005), multifunctional membranes (Zhao et al., 2010) and capsules (Gericke, Liebert, & Heinze, 2009), protein and gene delivery (Fayazpour et al., 2006; Park, Chun, Cho, & Song, 2010), molecular recognition and isolation (Harada & Kataoka, 1999), porous scaffolds for bone tissue (Coimbra et al., 2011), etc.

PECs are usually prepared in the dilute solution of polyelectrolytes. A change in solution concentration may significantly influence the interactions occurring in solutions. In the semidilute or concentrated solution and at the nonstoichiometric ratio of polyanions to polycations, the interaction between polyanions and polycations can lead to the formation of a three-dimensional network (Liu, Morishima, & Winnik, 2001). This is similar to the systems including oppositely charged polyelectrolyte and surfactant (Yang, Chen, & Fang, 2009). The reported polyelectrolyte systems in the semidilute or concentrated solutions were mainly those consisting of semisynthetic cationic cellulose and synthetical polyanions with lower molecular weight (Antunes, Lindman, & Miguel, 2005; Dreval', Vasil'ev, Litmanovich, & Kulichikhin, 2008; Liu et al., 2001; Liu, Morishima, & Winnik, 2002, 2003; Rodríguez, Alvarez-Lorenzo, & Concheiro, 2001; Thuresson, Nilsson, & Lindman, 1996; Tsianou, Kjøniksen, Thuresson, & Nyström, 1999); some including natural polysaccharides and proteins were also reported, but the research on them was not systematic enough (Chaisawang & Suphantharika, 2005; Marguerite, 2008; Taylor, Pearson, Draget, Dettmar, & Smidsrød, 2005; Wang, Qiu, Cosgrove, & Denbow, 2009). In our past work (Li, Hou, & Li, 2012), the electrostatic and hydrogen bonding interactions between xanthan gum (XG) and JR400, a natural polysaccharide and a semisynthetic cationic cellulose, in the semidilute and concentrated solutions were investigated and emphasis was placed on the influences of composition ratio and total solution concentration on these interactions. It was found that the viscosity of XG/JR400 mixture could be enhanced after mixing of XG and JR400 in an appropriate range of composition ratio and total concentration. In this paper, we investigated systematically the effects of composition, shear rate, pH and electrolyte on the rheological properties of

* Corresponding author. Tel.: +86 0531 88365460; fax: +86 0531 88364750.
E-mail address: wghou@sdu.edu.cn (W. Hou).

0144-8617/$ – see front matter © 2012 Elsevier Ltd. All rights reserved.
http://dx.doi.org/10.1016/j.carbpol.2012.07.001

aqueous solution of XG/JR400, which will help us get a better and more exhaustive insight into the interaction between XG and JR400 and the rheology of their mixed solutions.

XG is an anionic extracellular heteropolysaccharide secreted by *Xanthomonas campestris*, consisting of β-1,4-linked glucopyranose with trisaccharide side chains composed of D-mannose/D-glucuronic acid/D-mannose linked to alternate glucose residues. The D-mannose linked to the main chain contains an acetyl group at position O-6. The degree of acetylation at O-6 of mannose residue and substitution of pyruvate group at the terminal mannose residue depends on the fermentation condition (Krstonosic, Dokic, & Milanovic, 2011; Shobha & Tharanathan, 2009). XG solution has high-intrinsic viscosity and a pronounced pseudoplastic flow at relatively low concentrations due to its high molecular weight and the formation of aggregates via hydrogen bonds (Argin-Soysal, Kofinas, & Lo, 2009; Southwick, Lee, Jamieson, & Blackwell, 1980), which makes it suitable as thickener and stabilizer of emulsions or suspensions (Shen, Wan, & Gao, 2010). On mixing XG and other polymers, the hydrogen bonding and electrostatic interactions may turn up (Argin-Soysal et al., 2009; Chaisawang & Suphantharika, 2005; Lii, Liaw, Lai, & Tomasik, 2002). JR400 is the chloride salt of a trimethylammonium derivative of hydroxyethylcellulose. It functions as cationic, water-soluble and substantive conditioners for hair and skin care products (Liu et al., 2006). It is expected that the XG/JR400 mixture with higher viscosity should be better used as a thickener, stabilizer, etc. So this work is of both fundamental and practical importance.

2. Experimental

2.1. Materials

XG and JR400 were purchased from Aladdin (China) and Chongqing Haiyue Chemical Industry Co., Ltd. (China), respectively. More information about the samples has been provided in our past work (Li et al., 2012). Water was purified with a Hitech-Kflow water purification system (China). All other reagents are of analytical grade.

2.2. Solution preparation

The stock solutions (1%) of XG and JR400 were gained by dissolving 4.0 g of XG and JR400 in 396 g of H_2O, respectively. The XG and JR400 solutions at lower concentrations were obtained via the dilution of the stock solutions. Mixed solutions of XG and JR400 were prepared from weighed aliquots of the stock solutions. They were stirred for 12 h after mixing, and the stirring speed was adjusted to be as high as possible without forming any bubble. Finally, the mixtures were allowed to stand for 48 h at 25 °C. The pH values of the mixtures were adjusted with 0.1 M HCl and NaOH solutions while the NaCl concentration with 1% NaCl solution.

The ratio between the two components of the mixed solution, f_{JR}, is expressed as the weight fraction of JR400 in the mixture:

$$f_{IR} = \frac{W_{JR}}{W_{XG} + W_{JR}} \quad (1)$$

where W_{XG} and W_{JR} are the weights of the XG and JR400 stock solutions, respectively.

2.3. Methods

The rheological measurements of all the samples were carried out by a RS 75 rheometer (Haake Inc., Germany) equipped with the Z41 concentric cylinder system at 25.0 ± 0.1 °C. Every sample was rested for 20 min before measurement.

Dynamic measurements were carried out as follows: the stress sweep at the frequency (f) of 0.5 Hz was conducted from 0 to 10 Pa to determine the linear viscoelastic region. The frequency sweep was performed from 0.05 to 50 Hz at the stress of 0.05 Pa (in the linear viscoelastic region).

Steady viscosity at a constant shear rate and dynamic viscosity at 0.01 Hz and 0.05 Pa were obtained by measuring the viscosities that did not change any more with time.

Creep tests were carried out as follows: at time $t = 0$, a constant shear stress of 0.05 Pa was applied to the solutions and the compliance (J_t) was recorded as a function of t.

3. Results and discussion

3.1. Influence of composition ratio on dynamic modulus

The dynamic modulus can be influenced obviously by the composition ratio in the semidilute or concentrated solutions containing oppositely charged polyelectrolytes (Antunes et al., 2005; Liu et al., 2002, 2003; Marguerite, 2008; Thuresson et al., 1996; Tsianou et al., 1999). As was reported in our past work (Li et al., 2012), the stability map of XG/JR400 mixture can be divided into three regions: two stable regions (Regions I and II) and a flocculation region. Fig. 1 shows the effect of frequency on the dynamic storage and loss modulus (G' and G'') of XG/JR400 mixture with a total concentration (c_t) of 1% as f_{JR} changes in Regions I and II, respectively. It can be seen that both G' and G'' increase with f in the investigated range of 0.05–100 Hz. As f_{JR} increases from 0 to 0.40 in Region I and reduced from 1 to 0.78 in Region II, both G' and G'' increase initially and decrease subsequently. At f_{JR} less than 0.30 in Region I (Fig. 1a), the fluids present the features of typical physical gels: (1) over the entire frequency range (0.05–100 Hz) studied, G' values are higher than G'' values and no crossover is displayed between G' and G''; (2) both G' and G'' follow a power law in frequency of nearly identical exponent (G' and $G'' \sim \omega^n$, $\omega = 2\pi f$) (see Table S1 in supporting information); (3) the phase angle (δ) values are almost independent of f over the entire f range (Liu et al., 2003) (see Fig. S1 in supporting information). Actually, the physical gels here are weak gels rather than true gels since tan(δ) is greater than 0.1 (Schorsch, Garnier, & Doublier, 1997). The XG/JR400 mixture at $f_{JR} = 0.40$ shows viscoelastic behavior since a crossover between G' and G'' is observed (Fig. 1a). At low frequencies, the mixture behaves as a viscous fluid ($G'' > G'$) but became elastic ($G' > G''$) at frequencies higher than the crossover frequency. Moreover, both G' and G'' increase with f_{JR} at $0 < f_{JR} < 0.06$ while decrease with f_{JR} at $0.06 < f_{JR} < 0.40$. The former is due to the formation of three dimensional networks or gel structures arising from the electrostatic attraction and hydrogen bonds between XG and JR400; and the latter may be attributed to the partially destruction of the network structures arising from the formation of some XG/JR400 aggregates (Li et al., 2012).

In Region II (Fig. 1b and c), the pure JR400 solution ($f_{JR} = 1$) is typical Newtonian fluids with $G' \sim \omega^2$, $G'' \sim \omega^1$ (see Table S1 in supporting information), and $G'' > G'$ over the entire f domain studied (0.05–10 Hz) (Liu et al., 2002, 2003). The concentration of JR400 solution is well above the dilute regime (<0.28%) (Li et al., 2012). The formation of a transient network resulting from interchain entanglements of JR400 molecules (Liu et al., 2002) causes the weak elastic response of the solution. The mixture at $f_{JR} > 0.98$ is a viscous fluid with $G' < G''$ in the whole investigated frequency range. As f_{JR} decreases to the range of 0.90–0.78, the mixture turns into viscoelastic fluid with crossover of G' and G'' profile observed (Fig. 1b and c). The viscoelastic behavior here is different from that of the mixture at $f_{JR} = 0.40$. At low frequencies, the mixture here is

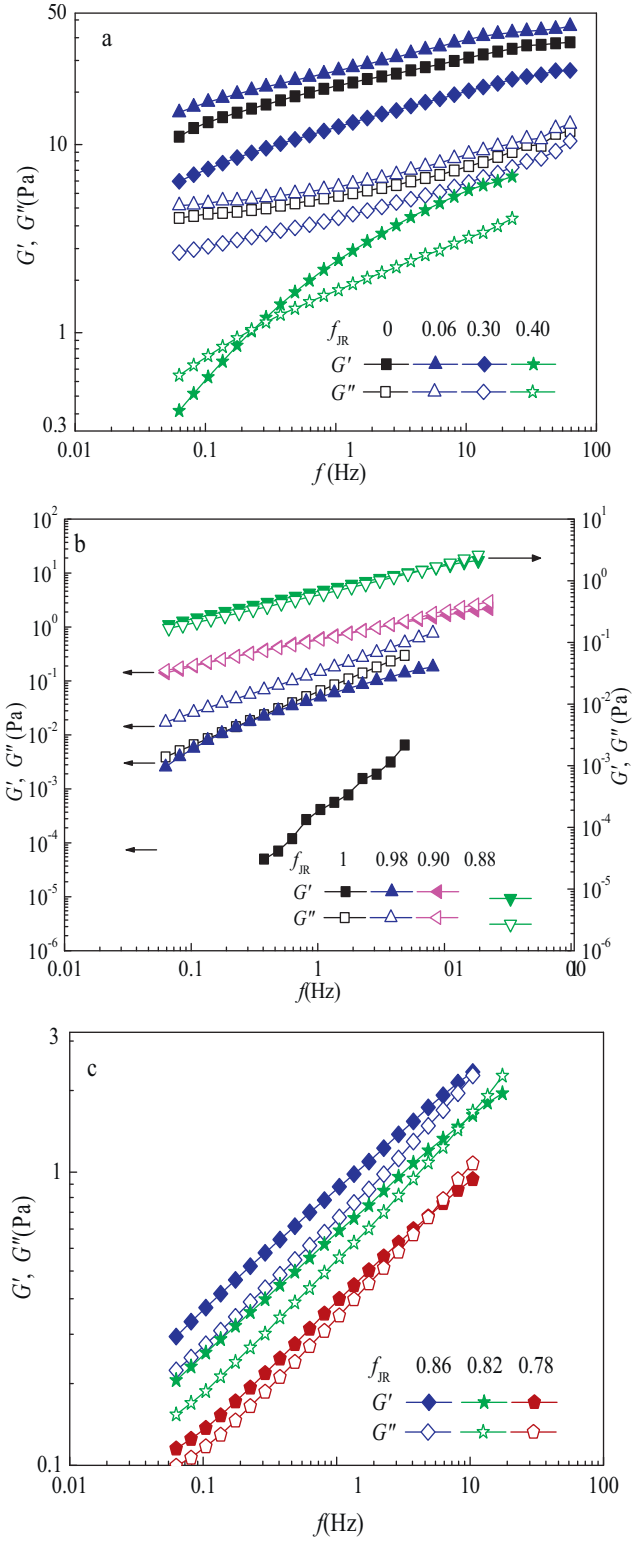

Fig. 1. Dependence of dynamic modulus on frequency for XG/JR400 mixture with total concentration of 1% and different f_{JR} (pH 6.40 ± 0.10).

dominantly elastic ($G' > G''$) while the mixture at $f_{JR} = 0.40$ dominantly viscous ($G' < G''$); at frequencies greater than the crossover frequency (f_c), the mixture here is dominantly viscous ($G' < G''$) while the mixture at $f_{JR} = 0.40$ dominantly elastic ($G' > G''$). For the mixture here, approximate power law relationship can be obtained: $G' \sim \omega^m$, $G'' \sim \omega^n$ (see Table S1 in supporting information). Meanwhile, it can be seen that f_c increases initially and decreases then

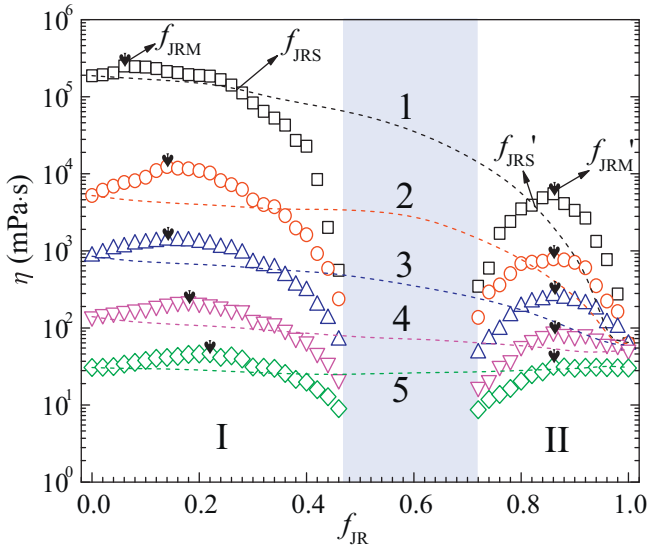

Fig. 2. Dependence of viscosity of XG/JR400 mixtures on f_{JR} at total concentration of 1% and different shear rate (pH 6.40 ± 0.10): □, 0.02π rad s^{-1}; ○, 1 s^{-1}; △, 10 s^{-1}; ▽, 100 s^{-1}; ◇, 1000 s^{-1}. Dash lines 1–5 show ideal viscosity of mixtures at shear rate of 0.02π rad s^{-1}, 1 s^{-1}, 10 s^{-1}, 100 s^{-1} and 1000 s^{-1}, respectively.

with f_{JR} decreasing, and the higher dynamic modulus corresponds to greater f_c or smaller characteristic relaxation time ($t_0 = 1/(2\pi f_c)$) (Fig. 1b and c). Usually, smaller f_c or longer characteristic relaxation time means stronger network structure, indicating higher viscosity or modulus of solutions (Liu et al., 2002, 2003), which applies to the XG/JR400 mixture in Region I (Fig. 1a). The abnormal phenomenon in Region II (Fig. 1b and c) cannot be interpreted to our knowledge now.

In addition, none of the G' and G'' profiles of XG/JR400 mixture displaying viscoelastic behavior (Fig. 1) can be fitted well with the single-mode Maxwell model. This is commonly seen in the associating polymers or two-component systems (Liu et al., 2002, 2003; Tam, Jenkins, Winnik, & Bassett, 1998), demonstrating that there is more than one relaxation process (Liu et al., 2003) for XG/JR400 mixture.

On the whole, the XG/JR400 mixture transforms from an elastic fluid into a viscoelastic fluid as f_{JR} increases in the investigated range of 0–0.40 (Region I), while from a viscous fluid into a viscoelastic fluid as f_{JR} decreases in the investigated range of 1–0.78 (Region II).

3.2. Influence of shear rate

Fig. 2 shows the influence of shear rate and dynamic frequency on the steady shear viscosity and dynamic viscosity (0.01 Hz), respectively, of the XG/JR400 mixtures at c_t of 1% and different f_{JR}. Ideal viscosity means the sum of viscosity of XG solution with concentration of $(1 - f_{JR})$% and that of JR400 solution with the corresponding concentration of f_{JR}%. As is depicted in our past work (Li et al., 2012), if the real viscosity of mixture is greater than the ideal one, it is considered that the mixing leads to a viscosity-increasing effect; on the contrary, the mixing leads to a viscosity-decreasing effect.

f_{JRM} and f_{JRM}' are used to symbolize the f_{JR} values where the viscosity reaches the maximum values, while f_{JRS} and f_{JRS}' symbolize the f_{JR} values where the real viscosity curves intersect the corresponding ideal ones (dash lines) in Region I and Region II, respectively, as is shown in Fig. 2. With f_{JR} increasing in Region I or decreasing in Region II, the viscosity of the mixture increases initially and decreases subsequently at each shear rate, which is in

accordance with our previous result (Li et al., 2012). As the shear rate is raised, the viscosity of the mixture decreases gradually both in Regions I and II. At every shear rate, the mixing leads to the viscosity enhancement at $0 < f_{JR} < f_{JRS}$ or $f_{JRS}' < f_{JR} < 1$, but causes the viscosity to decrease at $f_{JRS} < f_{JR} < 0.47$ or $0.71 < f_{JR} < f_{JRS}'$. It can be seen that f_{JRM} and f_{JRS} increase and f_{JRS}' decreases with the increase of shear rate, while the change of f_{JRM}' is not obvious. Similar tendency is observed for the mixture at c_t of 0.5% and 0.2% (see Figs. S2 and S3 in supporting information).

After mixing of XG and JR400 solutions at a constant total concentration, the electrostatic and hydrogen bonding interactions between XG and JR400 can increase the viscosity of XG/JR400 mixture, while the formation of some XG/JR400 aggregates causes the decrease of viscosity (Li et al., 2012). With the increase of shear rate, the electrostatic interaction and hydrogen bonds among the mixture will be destroyed partially (Scheme 1) (Thuresson et al., 1996). This leads to the viscosity decrease of the system. In addition, the increase of shear rate will prohibit the formation of XG/JR400 aggregates and, therefore, induces the gradual increase of f_{JRM} and f_{JRS} and decrease of f_{JRS}'.

3.3. Influences of pH

Fig. 3 shows the creep curves of 0.2% XG/JR400 mixture ($f_{JR} = 0.15$) at different pH. The creep curves of 0.17% XG solution at different pH show similar tendency and are not shown here (see Fig. S4 in supporting information). All the creep curves can be well described by Burger model consisting of two springs and two dashpots (Thünemann et al., 2004; Wyatt & Liberatore, 2009; Yang et al., 2009; Zakaria & Rahman, 1996) (see Table S2 in supporting information):

$$J_t = \frac{1}{E_0} + \frac{1}{E_1} \cdot (1 - e^{-t/t_0}) + \frac{t}{\eta_0} \quad (2)$$

where J_t (Pa^{-1}) is the compliance at time t, E_0 (Pa) the instantaneous elastic modulus, E_1 (Pa) the retarded elastic modulus, t_0 (s) the relaxation time and η_0 (Pa s) the zero-shear viscosity. The values of E_0, E_1, t_0 and η_0 can be determined by fitting with a nonlinear least-squares method via the software of Origin (Version 8.6).

Fig. 4 displays the real and ideal viscosities of the XG/JR400 mixture ($f_{JR} = 0.15$). The viscosity in this figure includes η_0 and the steady viscosity at different shear rate. The ideal viscosity here is the sum of viscosity of 0.17% XG solution and that of 0.03% JR400 solution. Both the real and ideal viscosity of XG/JR400 mixture increase at pH less than 5, keep almost constant at pH 5–10 and decrease at pH greater than 10 as pH increases from 2 to 12. In the investigated pH range, the real viscosity of XG/JR400 mixture is higher than the ideal one at pH greater than 2 and less than 12, showing a mixing-induced viscosity-increasing effect. Especially, the viscosity keeps almost stable and the viscosity enhancement is obvious at pH 5–10. Fig. 5 indicates the variation of the ideal and real values of E_0, E_1 and t_0 with pH for XG/JR400 mixture ($f_{JR} = 0.15$) at the total concentration of 0.2%. Greater E_0 and E_1 reflect the greater hardness and elasticity of investigated systems, respectively (Xu,

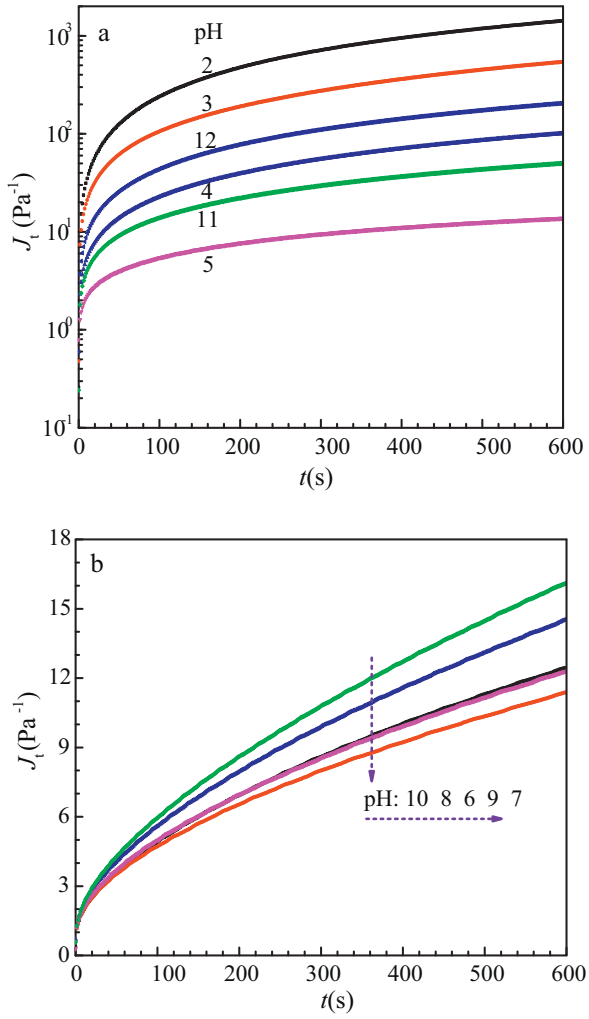

Fig. 3. Creep curves of 0.2% XG/JR400 mixture ($f_{JR} = 0.15$) at different pH.

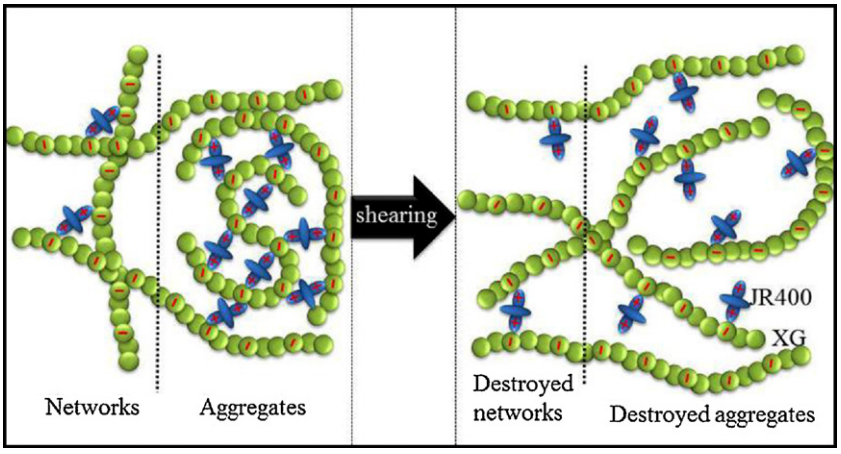

Scheme 1. Schematic drawing to illustrate effect of shearing on microstructures of XG/JR400 mixture.

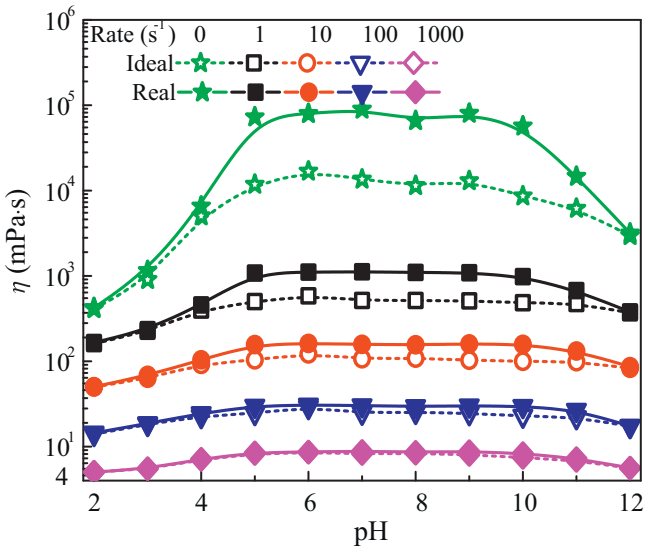

Fig. 4. Variation of ideal and real values of zero shear viscosity and steady viscosity at different shear rate with pH at total solution concentration of 0.2% for XG/JR400 mixture (f_{JR} = 0.15).

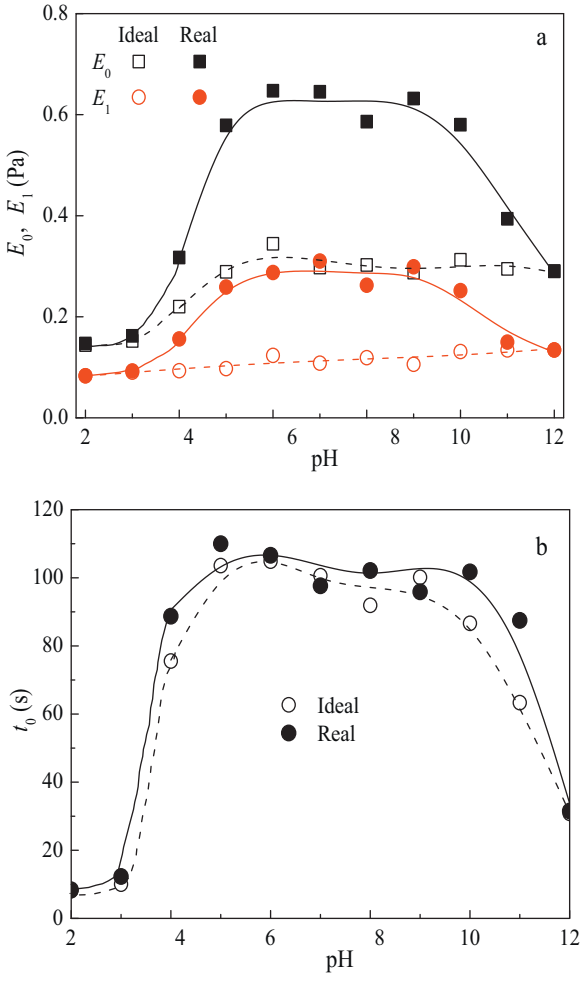

Fig. 5. Change of ideal and real values of (a) E_0, E_1 and (b) t_0 with pH for XG/JR400 mixture (f_{JR} = 0.15) at total concentration of 0.2%.

Xiong, Li, & Zhao, 2008). In general, E_0 and E_1 are used together to reflect the elastic strength of solutions or dispersions. It can be seen from Fig. 5a that the changing tendency of real E_0 and E_1 and ideal E_0 with pH is similar to that of η_0, but the ideal E_1 is almost constant at pH 2–12. In the investigated pH range, E_0 is always greater than E_1. The relaxation time t_0 is the time required for the strain of structural elements associated with viscoelastic behavior to reach $(1 - e^{-1})$ of their maximum strain (Wu et al., 2010). Longer relaxation time indicates that the viscoelastic behavior is sustained over longer periods (Xu et al., 2008). As is seen in Fig. 5, both the ideal and real t_0 increase at pH 2–5, nearly keep constant at pH 5–10 and decrease at pH 10–12 as pH is raised from 2 to 12. In the whole pH range, the real t_0 is slightly higher than the ideal one.

At pH about 2, nearly all the carboxyl groups exist as –COOH and the electrostatic interaction between XG and JR400 is quite weak, so the viscosity and elasticity of the XG/JR400 mixture is not enhanced obviously after mixing of XG and JR400 solutions. As pH increases from 2 to 5, the ionization degree of carboxyl groups is increased slightly, which makes XG molecules become more extended just like the polysaccharide extracted from *Prosopis africana* seeds (Achi & Okolo, 2004). These lead to the increment of viscosity, elasticity (E_0 and E_1) and t_0 of XG/JR400 mixture with pH increasing. The raised amount of $-COO^-$ also causes the increment of electrostatic interaction between XG and JR400, which strengthens the microstructures of the mixture. This leads to the higher real viscosity, elasticity and t_0 than the ideal ones (Figs. 4 and 5). At pH 5–10, maybe the electrostatic and hydrogen bonding interactions between XG and JR400 are almost constant, which makes the viscosity, elasticity and t_0 of XG/JR400 mixture nearly changeless in this pH range. But the hydrogen bonding and electrostatic interactions between XG and JR400 render the real viscosity, elasticity and t_0 of mixture greater than the ideal ones (Figs. 4 and 5). At pH 10–12, the carboxylic acid is completely disassociated (Liou, Chen, & Liu, 2003). The screening effect of added alkali on $-COO^-$ groups and alkaline depolymerization reactions (BeMiller, 1986) can weaken the hydrogen bonding and electrostatic interactions (Chen & Morawetz, 1983; Thuresson et al., 1996), so the viscosity, elasticity and t_0 of XG/JR400 mixture decrease. This also causes the viscosity and elasticity enhancement of mixture to turns less obvious with pH increasing in this pH range after mixing (Figs. 4 and 5). The pH-sensitivity of this mixture may make it used as cosmetics, drug dosage forms or to prepare mechanical sensors sensitive to external stimuli (Rodríguez et al., 2001).

3.4. Influence of electrolyte

The creep curves of 0.17% XG solution and XG/JR400 mixture with total concentration of 0.2% (f_{JR} = 0.15) at pH 6.40 ± 0.10 and different NaCl concentration (C_{NaCl}) are similar to Fig. 3 and not shown here (see Figs. S5 and S6 in supporting information). Fig. 6 shows the variation of ideal and real viscosity of 0.2% XG/JR400 mixture with C_{NaCl} at different shear rate. Fig. 7 depicts the change of real and ideal values of E_0 and E_1 of the mixture with C_{NaCl}. It can be seen from Figs. 6 and 7 that the ideal viscosity, E_0 and E_1 are slightly decreased while the real ones are obviously reduced as C_{NaCl} increases from 0 to 0.2%. At about $0 < C_{NaCl} < 0.1\%$, the real viscosity, E_0 and E_1 are greater than the ideal ones, but at $C_{NaCl} > 0.1\%$, the former is almost equal to the latter. The change of t_0 with C_{NaCl} is indistinct and not shown here (see Table S3 in supporting information).

The decreases of viscosity and elasticity of the mixture with increasing C_{NaCl} are caused by the screening effect of NaCl (like the alkali at pH greater than 10) (Chen & Morawetz, 1983; Thuresson et al., 1996) on the electrostatic and hydrogen bonding interactions between XG and JR400. Also, this screening effect induces the disappearance of the viscosity-increasing effect.

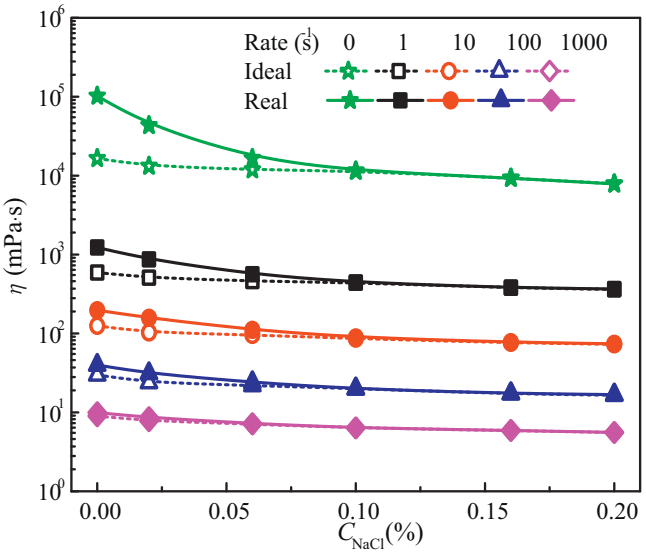

Fig. 6. Variation of ideal and real values of zero shear viscosity and steady viscosity at different shear rate with NaCl concentration at total solution concentration of 0.2% and pH 6.40 ± 0.10 for XG/JR400 mixture (f_{JR} = 0.15).

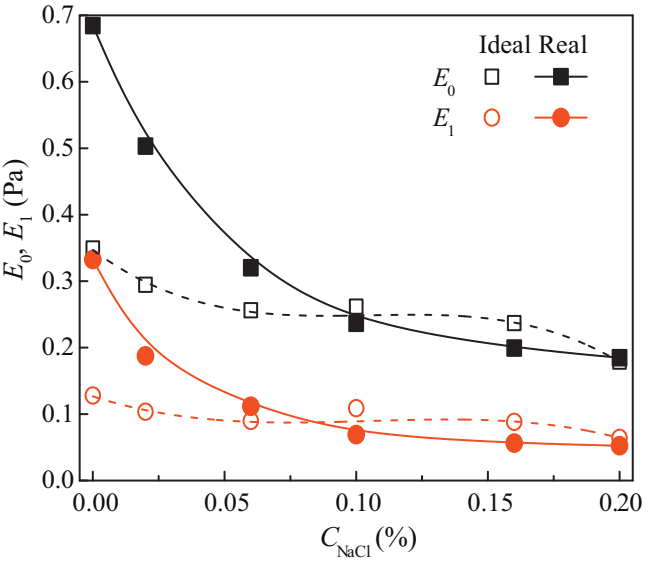

Fig. 7. Change of ideal and real values of E_0 and E_1 with NaCl concentration for XG/JR400 mixture (f_{JR} = 0.15) at total concentration of 0.2% (pH 6.40 ± 0.10).

As is discussed above, the raised shear rate can destroy both electrostatic and hydrogen bonding interactions severely. Therefore, the change of solution viscosity with composition ratio, pH and NaCl concentration turns unconspicuous at high shear rate, i.e. the effects of composition ratio, pH and NaCl concentration on the interactions between XG and JR400 are weakened as the shear rate increases (Figs. 4 and 6).

4. Conclusions

In this work, the effects of composition ratio, shear rate, pH and electrolyte concentration on the rheological properties of aqueous solution containing xanthan gum (XG) and cationic cellulose JR400 were investigated. It was found that the mixing of these two polymers can induce a viscosity-increasing effect for the mixed solution. At pH 5–10, both the viscosity and elasticity of the XG/JR400 mixture (f_{JR} = 0.15) are independent of pH and the viscosity-increasing effect is obvious. Outside this pH range, the viscosity, elasticity and viscosity-increasing effect of the mixture decrease. The addition of NaCl and increase of the shear rate can induce the decrease of viscosity, elasticity and viscosity-increasing effect of the XG/JR400 mixture.

Acknowledgements

This work was financed by the National Natural Science Foundation of China (No. 21173135), the Specialized Research Fund for the Doctoral Program of Higher Education of China (No. 20110131130008) and Taishan Scholar Foundation of Shandong Province of China (No. ts20070713).

Appendix A. Supplementary data

Supplementary data associated with this article can be found, in the online version, at http://dx.doi.org/10.1016/j.carbpol.2012.07.001.

References

Achi, O. K., & Okolo, N. I. (2004). The chemical composition and some physical properties of a water-soluble gum from *Prosopis africana* seeds. *International Journal of Food Science & Technology*, *39*, 431–436.
Al-Jamal, K. T., Ramaswamy, C., & Florence, A. T. (2005). Supramolecular structures from dendrons and dendrimers. *Advanced Drug Delivery Reviews*, *57*, 2238–2270.
Antunes, F. E., Lindman, B., & Miguel, M. G. (2005). Mixed systems of hydrophobically modified polyelectrolytes: Controlling rheology by charge and hydrophobe stoichiometry and interaction strength. *Langmuir*, *21*, 10188–10196.
Argin-Soysal, S., Kofinas, P., & Lo, Y. M. (2009). Effect of complexation conditions on xanthan–chitosan polyelectrolyte complex gels. *Food Hydrocolloids*, *23*, 202–209.
BeMiller, J. N. (1986). An introduction to pectins – Structure and properties. *ACS Symposium Series*, *310*, 2–12.
Chaisawang, M., & Suphantharika, M. (2005). Effects of guar gum and xanthan gum additions on physical and rheological properties of cationic tapioca starch. *Carbohydrate Polymers*, *61*, 288–295.
Chen, H. L., & Morawetz, H. (1983). Fluorometric study of the equilibrium and kinetics of poly(acrylic acid) association with polyoxyethylene or poly(vinyl pyrrolidone). *European Polymer Journal*, *19*, 923–928.
Coimbra, P., Ferreira, P., de Sousa, H. C., Batista, P., Rodrigues, M. A., Correia, I. J., et al. (2011). Preparation and chemical and biological characterization of a pectin/chitosan polyelectrolyte complex scaffold for possible bone tissue engineering applications. *International Journal of Biological Macromolecules*, *48*, 112–118.
Dinu, I. A., Mihai, M., & Dragan, E. S. (2010). Comparative study on the formation and flocculation properties of polyelectrolyte complex dispersions based on synthetic and natural polycations. *Chemical Engineering Journal*, *160*, 115–121.
Doi, R., & Kokufuta, E. (2010). On the water dispersibility of a 1:1 stoichiometric complex between a cationic nanogel and linear polyanion. *Langmuir*, *26*, 13579–13589.
Dreval', V., Vasil'ev, G., Litmanovich, E., & Kulichikhin, V. (2008). Rheological properties of concentrated aqueous solutions of anionic and cationic polyelectrolyte mixtures. *Polymer Science Series A*, *50*, 751–756.
El-Hag Ali Said, A. (2005). Radiation synthesis of interpolymer polyelectrolyte complex and its application as a carrier for colon-specific drug delivery system. *Biomaterials*, *26*, 2733–2739.
Fayazpour, F., Lucas, B., Alvarez-Lorenzo, C., Sanders, N. N., Demeester, J., & De Smedt, S. C. (2006). Physicochemical and transfection properties of cationic hydroxyethylcellulose/DNA nanoparticles. *Biomacromolecules*, *7*, 2856–2862.
Fuoss, R. M., & Sadek, H. (1949). Mutual interaction of polyelectrolytes. *Science*, *110*, 552–554.
Gericke, M., Liebert, T., & Heinze, T. (2009). Polyelectrolyte synthesis and in situ complex formation in lonic liquids. *Journal of the American Chemical Society*, *131*, 13220–13221.
Harada, A., & Kataoka, K. (1999). Chain length recognition: Core–shell supramolecular assembly from oppositely charged block copolymers. *Science*, *283*, 65–67.
Kötz, J., Kosmella, S., & Beitz, T. (2001). Self-assembled polyelectrolyte systems. *Progress in Polymer Science*, *26*, 1199–1232.
Kabanov, A. V., & Kabanov, V. A. (1998). Interpolyelectrolyte and block ionomer complexes for gene delivery: Physico-chemical aspects. *Advanced Drug Delivery Reviews*, *30*, 49–60.
Kabanov, V. A. (2005). Polyelectrolyte complexes in solution and in bulk. *Russian Chemical Reviews*, *74*, 3–20.
Krstonosic, V., Dokic, L., & Milanovic, J. (2011). Micellar properties of OSA starch and interaction with xanthan gum in aqueous solution. *Food Hydrocolloids*, *25*, 361–367.

Li, H., Hou, W., & Li, X. (2012). Interaction between xanthan gum and cationic cellulose JR400 in aqueous solution. *Carbohydrate Polymers*, *89*, 24–30.
Lii, C. Y., Liaw, S. C., Lai, V. M. F., & Tomasik, P. (2002). Xanthan gum–gelatin complexes. *European Polymer Journal*, *38*, 1377–1381.
Liou, S., Chen, S., & Liu, D. (2003). Synthesis and characterization of needlelike apatitic nanocomposite with controlled aspect ratios. *Biomaterials*, *24*, 3981–3988.
Liu, R. C. W., Morishima, Y., & Winnik, F. M. (2001). A rheological evaluation of the interactions in water between a cationic cellulose ether and sodium poly(2-acrylamido-2-methylpropanesulfonates). *Macromolecules*, *34*, 9117–9124.
Liu, R. C. W., Morishima, Y., & Winnik, F. M. (2002). Rheological properties of mixtures of oppositely charged polyelectrolytes. A study of the interactions between a cationic cellulose ether and a hydrophobically modified poly[sodium 2-(acrylamido)-2-methylpropanesulfonate]. *Polymer Journal*, *34*, 340–346.
Liu, R. C. W., Morishima, Y., & Winnik, F. M. (2003). Composition-dependent rheology of aqueous systems of amphiphilic sodium poly(2-acrylamido-2-methylpropanesulfonates) in the presence of a hydrophobically modified cationic cellulose ether. *Macromolecules*, *36*, 4967–4975.
Liu, X. M., Gao, W., Maziarz, E. P., Salamone, J. C., Duex, J., & Xia, E. (2006). Detailed characterization of cationic hydroxyethylcellulose derivatives using aqueous size-exclusion chromatography with on-line triple detection. *Journal of Chromatography A*, *1104*, 145–153.
Marguerite, R. (2008). Rheological investigation on hyaluronan-fibrinogen interaction. *International Journal of Biological Macromolecules*, *43*, 444–450.
Michaels, A. S. (1965). Polyelectrolyte complexes. *Industrial & Engineering Chemistry*, *57*, 32–40.
Michaels, A. S., & Miekka, R. G. (1961). Polycation–polyanion complexes: Preparation and properties of poly(vinylbenzyltrimethylammonium)/poly(styrenesulfonate). *The Journal of Physical Chemistry*, *65*, 1765–1773.
Michaels, A. S., Mir, L., & Schneider, N. S. (1965). A conductometric study of polycation–polyanion reactions in dilute aqueous solution. *The Journal of Physical Chemistry*, *69*, 1447–1455.
Park, M. R., Chun, C. J., Cho, C. S., & Song, S. C. (2010). Enhancement of sustained and controlled protein release using polyelectrolyte complex-loaded injectable and thermosensitive hydrogel. *European Journal of Pharmaceutics and Biopharmaceutics*, *76*, 179–188.
Rodríguez, R., Alvarez-Lorenzo, C., & Concheiro, A. (2001). Rheological evaluation of the interactions between cationic celluloses and carbopol 974P in water. *Biomacromolecules*, *2*, 886–893.
Schorsch, C., Garnier, C., & Doublier, J.-L. (1997). Viscoelastic properties of xanthan/galactomannan mixtures: Comparison of guar gum with locust bean gum. *Carbohydrate Polymers*, *34*, 165–175.
Shen, D., Wan, C., & Gao, S. (2010). Molecular weight effects on gelation and rheological properties of konjac glucomannan-xanthan mixtures. *Journal of Polymer Science Part B: Polymer Physics*, *48*, 313–321.
Shobha, M. S., & Tharanathan, R. N. (2009). Rheological behaviour of pullulanase-treated guar galactomannan on co-gelation with xanthan. *Food Hydrocolloids*, *23*, 749–754.
Southwick, J. G., Lee, H., Jamieson, A. M., & Blackwell, J. (1980). Self-association of xanthan in aqueous solvent-systems. *Carbohydrate Research*, *84*, 287–295.
Tam, K. C., Jenkins, R. D., Winnik, M. A., & Bassett, D. R. (1998). A structural model of hydrophobically modified urethane-ethoxylate (HEUR) associative polymers in shear flows. *Macromolecules*, *31*, 4149–4159.
Taylor, C., Pearson, J. P., Draget, K. I., Dettmar, P. W., & Smidsrød, O. (2005). Rheological characterisation of mixed gels of mucin and alginate. *Carbohydrate Polymers*, *59*, 189–195.
Thünemann, A. F., Müller, M., Dautzenberg, H., Joanny, J. F., & Löwen, H. (2004). Polyelectrolyte complexes. In M. Schmidt (Ed.), *Polyelectrolytes with defined molecular architecture II* (pp. 19–33). Berlin/Heidelberg: Springer.
Thuresson, K., Nilsson, S., & Lindman, B. (1996). Effect of hydrophobic modification on phase behavior and rheology in mixtures of oppositely charged polyelectrolytes. *Langmuir*, *12*, 530–537.
Tsianou, M., Kjøniksen, A. L., Thuresson, K., & Nyström, B. (1999). Light scattering and viscoelasticity in aqueous mixtures of oppositely charged and hydrophobically modified polyelectrolytes. *Macromolecules*, *32*, 2974–2982.
Tsuchida, E., & Abe, K. (1982). Interactions between macromolecules in solution and intermacromolecular complexes. In E. Tsuchida, & K. Abe (Eds.), *Interactions between macromolecules in solution and intermacromolecular complexes* (pp. 1–119). Berlin/Heidelberg: Springer.
Wang, Y., Qiu, D., Cosgrove, T., & Denbow, M. L. (2009). A small-angle neutron scattering and rheology study of the composite of chitosan and gelatin. *Colloids and Surfaces B: Biointerfaces*, *70*, 254–258.
Wu, M., Li, D., Wang, L.-J., Özkan, N., & Mao, Z.-H. (2010). Rheological properties of extruded dispersions of flaxseed-maize blend. *Journal of Food Engineering*, *98*, 480–491.
Wyatt, N. B., & Liberatore, M. W. (2009). Rheology and viscosity scaling of the polyelectrolyte xanthan gum. *Journal of Applied Polymer Science*, *114*, 4076–4084.
Xu, Y., Xiong, S., Li, Y., & Zhao, S. (2008). Study on creep properties of indica rice gel. *Journal of Food Engineering*, *86*, 10–16.
Yang, J., Chen, S., & Fang, Y. (2009). Viscosity study of interactions between sodium alginate and CTAB in dilute solutions at different pH values. *Carbohydrate Polymers*, *75*, 333–337.
Zakaria, M. B., & Rahman, Z. A. (1996). Rheological properties of cashew gum. *Carbohydrate Polymers*, *29*, 25–27.
Zhao, Q., An, Q., Sun, Z., Qian, J., Lee, K. R., Gao, C., et al. (2010). Studies on structures and ultrahigh permeability of novel polyelectrolyte complex membranes. *The Journal of Physical Chemistry B*, *114*, 8100–8106.